A semi-automated, multi-source data fusion update of a wetland inventory for east-central Minnesota, USA

Steven M. Kloiber[1], Robb D. Macleod[2], Aaron J. Smith[3], Joseph F. Knight[4], and Brian J. Huberty[5]

1) Minnesota Department of Natural Resources (correponding author)
   500 Lafayette Road North
   St. Paul, MN 55155
   Phone: 651-259-5164 / FAX: 651-296-1811
   E-mail: steve.kloiber@state.mn.us

2) Ducks Unlimited Inc.
   1220 Eisenhower Place
   Ann Arbor, MI 48108

3) Equinox Analytics Inc.
   PO Box 6941
   Columbia, SC 29204

4) Department of Forest Resources
   University of Minnesota
   1530 Cleveland Ave N
   Saint Paul, MN 55108

5) U.S. Fish & Wildlife Service
   5600 American Blvd West; Suite 990
   Bloomington, MN 55437

ABSTRACT

Comprehensive wetland inventories are an essential tool for wetland management, but developing and maintaining an inventory is expensive and technically challenging. Funding for these efforts has also been problematic. Here we describe a large-area application of a semi-automated process used to update a wetland inventory for east-central Minnesota. The original inventory for this area was the product of a labor-intensive, manual photo-interpretation process. The present application incorporated high resolution, multi-spectral imagery from multiple seasons; high resolution elevation data derived from lidar; satellite radar imagery; and other GIS data. Map production combined image segmentation and random forest classification along with aerial photo-interpretation. More than 1000 validation data points were acquired using both independent photo-interpretation as well as field reconnaissance. Overall accuracy for wetland identification was 90% compared to field data and 93% compared to photo-interpretation data. Overall accuracy for wetland type was 72% and 78% compared to field and photo-interpretation data, respectively. By automating the most time consuming part of the image interpretations, initial delineation of boundaries and identification of broad wetland classes, we were able to allow the image interpreters to focus their efforts on the more difficult components, such as the assignment of detailed wetland classes and modifiers.

Keywords: wetlands inventory, wetland mapping, accuracy assessment, remote sensing

INTRODUCTION

Wetland inventory maps are essential tools for wetland management, protection, and restoration planning. They provide information for assessing the effectiveness of wetland policies and management actions. These maps are used at all levels of government, as well as by private industry and non-profit organizations for wetland regulation and management, land use and conservation planning, environmental impact assessment, and natural resource inventories. Wetland inventories are used to assess impacts of regulatory policy (Gwin et al. 1999), assess habitat distribution and quality (Austin et al. 2000; Hepinstall et al. 1996; Marchand and Litvaitis 2004; Knutson et al. 1999), evaluate carbon storage potential and climate change impacts (Euliss et al. 1999; Burkett and Kusler 2000), and measure and predict waterfowl and amphibian population distribution (Yerkes, et al. 2007; Munger et al. 1998; Knutson et al. 1999).

There are several notable efforts across the globe to conduct national and regional comprehensive wetland inventories. The Canadian Wetland Inventory (CWI) is developing a comprehensive wetland inventory based on remote sensing data from Landsat and Radarsat platforms (Li and Chen 2005; Fournier et al 2007). The CWI maps wetlands down to a minimum mapping unit of 1 ha using a five class system. In 1974, the U.S. Fish and Wildlife Service began an effort to implement the National Wetlands Inventory (NWI) for the United States (Cowardin et al. 1979). The NWI is based on manual aerial photo-interpretation with a target map unit of 0.2 ha and a detailed hierarchical classification scheme involving wetland systems, classes, subclasses, water regimes, and special modifiers (Dahl 2009). The Mediterranean wetland initiative promotes standardized methods for wetland inventory and monitoring across multiple countries in the Mediterranean region (Costa et al 2001). Wetland classification and mapping recommendations for this initiative closely follow the NWI. More recently, wetlands across China have been mapped using Landsat data into three broad classes with 15 subtypes generally based on landscape and landform characteristics (Gong et al. 2010). Despite these efforts, a review of the status of wetland inventories concluded that there still are significant gaps in our knowledge about the extent and condition of global wetland resources. Finlayson and Spiers (1999) found that outside of a few of the more developed countries and regions, wetland inventories were generally incomplete or non-existent.

Even regions with comprehensive wetland inventories require periodic updates. For example, in Minnesota, most of the NWI is 25 to 30 years old. Many changes in wetland extent and type have occurred since the original inventory was completed. Agricultural expansion and urban development have contributed to wetland loss. Conversely, various wetland conservation policies and programs have resulted in the restoration of some previously drained wetlands and the creation of new wetlands. Furthermore, limitations in the technology, methodology and source data for the original NWI resulted in an under representation of certain types of wetlands. In northeastern Minnesota, wetlands were originally mapped using 1:80,000 scale panchromatic imagery. The resulting wetland maps in this area tend to be very conservative, missing many forested and drier emergent wetlands (LMIC 2007). Updating the wetland inventory for such areas enhances the ability of conservation organizations to make better management decisions. There is a significant ongoing need to develop and update wetland inventories.

Maintaining wetland inventories can be expensive and technically challenging given the complexity of wetland features and user expectations for a high degree of accuracy. Federally funded updates to the NWI are required to conform to the federal wetland mapping standard (FGDC 2009). This standard calls for ≥98% producer's accuracy for all wetland features larger than 0.2 ha and a wetland class-level accuracy of ≥85%. Unfortunately, funding for mapping in the NWI program has declined over the past 20 years (Tiner 2009) and has been almost entirely eliminated as of 2014 (NSGIC 2014).

Historically, the NWI has been primarily the product of manual aerial photo-interpretation (Tiner 1990). Much of the original delineation and classification was done using hardcopy stereo imagery with mylar overlays. In the last decade, NWI mapping efforts have largely transitioned to heads-up, on-screen digitizing and classification from digital orthorectified imagery (Drazkowski et al 2004; Dahl et al. 2009). Despite the efficiency gains achieved by migrating to an on-screen digitizing process, the process is still labor-intensive.

Automated classification of wetlands from remote sensing data has had varied results. Ozesmi and Bauer (2002) compare the results of automated wetland classification using satellite imagery to wetland mapping from manual photo-interpretation. In their review, they note that the limitations of satellite imagery, specifically resolution limitations when compared to aerial photography as well as limitations related to spectral confusion between classes, led the NWI program to choose a method based on photo-interpretation. However, given the advancements in the fields of remote sensing and image analysis since the NWI was originally designed, the use of automated mapping and classification techniques warrants reconsideration.

Collecting, managing, and analyzing large quantities of high spatial resolution digital imagery has improved significantly over the past two or three decades. Airborne imagery acquisition systems like the Zeiss/Intergraph Digital Mapping Camera (Z/I DMC) and the Vexcel Ultracam are commonly used to acquire four-band multispectral imagery at less than 1-meter resolution. In addition, high-resolution, multispectral imagery is also available through various satellite systems such as Worldview-2, Quickbird and IKONOS. The costs for data storage required for the large quantities of high-resolution imagery data have dropped significantly and advances in automated image analysis techniques have improved the efficiency with which these data can be processed.

Radar imagery shows potential to provide new information such as water level changes in wetlands, soil saturation and vegetation structure (Corcoran et al. 2011; Bourgeau-Chavez et al. 2013). In the near term, the sources of satellite radar imagery are somewhat limited. Yet, Radarsat imagery is being used operationally as part of the Canadian Wetland Inventory (Brisco et al. 2008).

Recent widespread adoption of scanning topographic lidar systems also provides a new source of highly relevant digital information for wetland mapping. The distribution and occurrence of wetlands is heavily influenced by topography. For example, Beven and Kirkby (1979) described a topographic index to predict spatial patterns of soil saturation based on the ratio of the upslope catchment area to the tangent of the local slope. Numerous researchers have used this topographic index, alternately known as the compound topographic index (CTI) or the wetness index, to predict the occurrence of wetlands (Hogg and Todd 2007; Murphy et al. 2007; Rampi et al. 2014b). As such, topographic analysis of lidar data is an important emerging technology for wetland mapping.

Image segmentation is a process that groups adjacent image pixels into larger image objects based on criteria specified by the image analyst. The goal of segmentation is to simplify the image into a smaller number of potentially meaningful objects which can then be classified using various attributes describing these objects (i.e. brightness, texture, size, and shape). This technique simultaneously reduces data volume while incorporating spatial contextual information in the classification process. Image segmentation has been shown to be a potentially valuable technique for improving image classification accuracy for mapping land cover (Myint et al. 2011) and wetlands (Frohn et al. 2009).

Classification algorithms like random forest (Breiman 2001) have greatly improved our ability to effectively integrate data from multiple sources into an automated classification procedure. Incorporating data from multiple sensor systems as well as ancillary GIS data can potentially improve wetland classification accuracy (Corcoran et al. 2011, Knight et al. 2013, Corcoran et al. 2013, Rampi et al. 2014a).

Here we describe a large area application of a semi-automated classification process used to update the NWI. The objective of this effort was to determine whether automated techniques such as image segmentation, digital terrain analysis, and random forest classification could be combined with multiple high-resolution remote sensing and GIS data sets and traditional photo-interpretation to efficiently produce an accurate and spatially detailed wetland inventory map.

METHODS

Study Area

The study area is 18,520 square kilometers, centered on the 13-county metropolitan area of Minneapolis and Saint Paul, Minnesota (Figure 1). The study area is situated primarily in the Eastern Broadleaf Forest Ecological Province (DNR 2013) and the climate is typical of its continental position with hot summers and cold winters. Typical annual precipitation ranges from about 76 to 81 centimeters (Minnesota Climatology Working Group 2012). Land use in the study area varies from a dense urban core with a mix of commercial and high density residential area, to lower density suburban and exurban communities, and rural agricultural and forests.

Input Data

The primary imagery used for the NWI update was spring, leaf-off, digital aerial imagery with four spectral bands (red, green, blue, and near infrared) in 541 orthorectified USGS quarter quadrangle tiles. The imagery was acquired using a Z/I DMC camera in early April of 2010 and late April to early May of 2011. Imagery for 60% of the project area was acquired at a spatial resolution of 30 cm, while imagery for the other 40% was acquired at 50 cm resolution. The imagery has a horizontal root mean square error (radial) of 78 cm (MnGeo 2010). For the image segmentation process, the 30cm images were resampled to 50cm resolution using a bilinear interpolation algorithm.

Thirteen single-date scenes of PALSAR L-band radar were acquired to cover the project area to aid in the identification of forested wetlands. The scenes available were a combination of single and dual polarization during a leaf-off seasonal window. The Alaska Satellite Facility MapReady Remote Sensing Tool Kit (ASF 2011) was used for terrain correction and geo-referencing. Additional geo-referencing was performed in ArcGIS using control points selected from the aerial imagery. A radar processing extension in Opticks was used to reduce speckle in the data (Opticks 2011). Radar imagery was classified using a 10-class maximum-likelihood ISODATA clustering routine implemented in ERDAS Imagine software (ERDAS 2008). The classes associated with "wet forest" training sites were identified and the classification was applied to all clusters within the radar image.

Digital elevation models (DEMs) were derived from lidar data for approximately 60% of project area, while DEMs for the remainder were 10-meter resolution DEMs obtained from the National Elevation Dataset. The typical lidar point spacing was about 1 point per square meter. The Minnesota DNR processed the bare earth points into a digital elevation model using 3D Analyst for ArcGIS by importing the points into a terrain data set and then interpolating a 1-meter DEM that was subsequently resampled to a 3-meter DEM. This lidar DEM has a vertical root mean square of 18 cm.

ArcGIS Spatial Analyst (ESRI 2011) was used to calculate slope, curvature, plan curvature, profile curvature, topographic position index (TPI) and compound topographic index (CTI). TPI was calculated by subtracting the mean elevation for a given pixel from the mean elevation of its neighborhood (Guisan et al. 1999). We used an annulus neighborhood with radii of 15 and 20 meters. The CTI (Moore 1991) was calculated using a sinkless version of the DEM. A slope grid and upstream catchment area grid were calculated using the D-Infinity flow directions tool from TauDEM (Tarboton 2003). CTI was then computed from slope and contributing drainage area using a custom python script.

The Natural Resources Conservation Service (NRCS) digital Soil Survey Geographic (SSURGO) layers were compiled for the project area (NRCS 2010). Two derived raster products were produced from SSURGO data; (1) the soil water regime class, and (2) the percentage of hydric soil. The variables used to derive these products included drainage class, flood frequency for April, pond frequency for April, and pond frequency for August.

The layers described above were formatted for input to an Object Based Image Analysis (OBIA) process using the Cognition Network Language (CNL) implemented within eCognition software (Trimble 2010). Images were clipped to the boundary of the relevant quarter quad tile and stacked with ERDAS Imagine software (ERDAS 2008) into a single multi-layer file subsequently referred to here as the layer-stack.

Training Data

Reference field data were collected to serve as training data for the random forest classification and to guide the interpreters during the image interpretation process. A set of 12 representative sub-areas were selected for field visits to provide representative training data for the wetland types found throughout the project area. The sub-areas were selected to be spatially distributed and to represent the range of landscape types in the project area. Within these sub-areas, individual wetland sites were selected for field visits using a stratified-random sampling approach with strata proportioned according to the frequency of wetland classes. Rarely occurring wetland types were always flagged for field visits. A total of 510 field sites were visited. The training data were augmented by including 1967 sites selected from field data provided by field biologists at the Metropolitan Mosquito Control District as well as 873 sites image-interpreted by Ducks Unlimited.

All training data were classified according to the Cowardin classification system (Cowardin et al. 1979), which is a hierarchical system developed to standardize the classification of wetlands and deepwater habitats of the United States. Additional details of the classification system including the definition of each system, subsystem, class, and subclass can be found in Cowardin et al. (1979) and Dahl et al. (2009).

Automated Components

The object-based image analysis (OBIA) rule set consisted of several steps to separate wetlands from other land cover types. The process began with a multi-resolution segmentation algorithm (Baatz and Schape2000) that created image objects (groups of spectrally similar pixels). Parameters for the initial segmentation were; scale factor = 6, shape = 0.5, compactness = 0.9, RGB weight = 1, and near infrared weight = 2. A relatively small scale parameter was chosen to ensure that small wetlands would be represented in the lowest level of the image object hierarchy. A three-tier hierarchy consisting of spatially nested sub-objects, mid-level objects, and super objects provided a flexible framework for iteratively integrating information from different image and topographic data sources. The rule set was designed to draw boundaries for real world features of interest (e.g., stream beds) by iteratively aggregating sub-objects at a temporary mid-level according to rules defining specific features of interest for each major sequence of the larger rule set. Once useful boundaries for a particular sequence were identified (using temporary classification thresholds and modification of the object boundaries at the mid-level), the feature boundary information was conveyed to the super-level for inclusion in the final output. Each modified mid-level was then destroyed and the unmodified sub-objects were re-used to initialize a new version of the mid-level to repeat the process of selective aggregation and classification for the next feature of interest.

The first major process sequence was designed to identify wooded-wetlands using the PALSAR radar data. Sub-objects were aggregated at a temporary mid-level according to boundaries created from the previously classified PALSAR data. A mask layer with the boundaries of the PALSAR wetland clusters was incorporated into the layer stack data. The boundaries created by the 20m resolution PALSAR-derived wooded wetland mask were not cartographically compatible with boundaries for other features derived from the 0.5m resolution image data. This difference was reconciled in the eCognition rule set via a custom-built iterative pixel-based object merging and reshaping algorithm applied to the mid-level in the object hierarchy.

The second major process sequence in the rule set was designed to isolate open water stream features and stream-bed topographic features. A preliminary linear stream vector layer was generated using Arc Hydro terrain modeling software (Maidment 2002) to identify likely flow pathways using the lidar derived DEM data. This linear flow path layer was used to seed a region growing sequence that identified spectrally dark sub-objects contiguous to the modeled stream lines. These objects were merged at the mid-level and the boundaries were smoothed to form the stream polygons, which were then stored at the super-object level. A spectral difference segmentation algorithm (Definiens Imaging, 2009) was then used on the DEM (threshold value of 0.05m) to generate temporary elevation contours. The contour objects containing nested stream-sub-objects were then identified and classified as potential riparian areas, which were more likely to contain wetlands.

The third major process sequence in the rule set separated forested areas from non-forested areas and selectively generated contour lines in forest polygons. Forested areas were identified by aggregating sub-objects at a temporary mid-level according to image spectral characteristics ($0.017 < NDVI < 0.28$ and RGB brightness < 150) and textural characteristics (average mean difference to neighbors of sub-objects > 0.95 in the NIR band). Small candidate forest objects were then merged into stand sized forested objects. Based on prior experience, the photo interpretation team requested that elevation data be added to forested areas. A spectral difference algorithm which merged together objects with similar elevation values was applied to the sub-objects of the forest stand objects. An elevation threshold value of 0.33m was used to create objects that approximate 0.33m contour intervals.

The final major process sequence in the rule set was designed to create a background layer of general-purpose image objects, which are delivered to the photo-interpretation team for editing in order to create the final wetland map. A multi-resolution segmentation algorithm (parameters: scale factor = 400, shape = 0.1, compactness = 0.9, RGB weight = 1 and NIR weight = 2) was used in all areas not classified in the previous sequences to delineate strongly visible boundaries in the spring leaf-off imagery. This finalized set of image objects was then smoothed and exported in a vector shape-file format for transfer to the photo-interpretation team.

Each image object has numerous associated attributes derived from the imagery, DEM, and other ancillary data sets. These attributes, along with the training data, were used to create a classification model using the randomForest package in R (R Development Core Team 2011; Breiman 2001). All image objects were also assigned a unique identification number so that the classification model results could be linked back to the image objects.

Manual Components

A 750-meter square grid system (enabling the interpreter to completely view an image section on a monitor at 1:3,000) overlaid on each image was used to systematically guide image-interpretation efforts and ensure complete interpretation of each image. Interpreters viewed the classified image segmentation data superimposed over the spring imagery to identify and categorize wetlands. Additional ancillary data were used during the interpretation process when needed, including~~;~~ summer imagery from 2008-2010, SSURGO soils derived products, the DEM, and DEM derived products. The interpreters could use the segmentation derived boundary without modification, manually edit the polygon boundary, or discard the segmentation based boundary to manually digitize a new boundary.

Adjacent wetland polygons of the same class were merged. All automated wetland classification values were either confirmed or manually reclassified by a human interpreter. As with the field data, all mapped wetland polygons were classified according to the Cowardin classification system (Table 1).

Validation Data

Two sets of independent validation data were created using field checks and independent image-interpretation, respectively. The validation data were not made available to the image analysts. These data were reserved to make a post-processing accuracy assessment of the updated wetland inventory maps.

We created a set of 951 validation points through field checks and another set of 901 validation points through independent image-interpretation. All points were initially selected using a stratified-random sampling process with the strata defined by a recently developed land cover dataset from the Minnesota wetland status and trends monitoring program (Kloiber et al. 2012). The stratification was designed to place 75% of the selected points in wetlands and 25% in uplands. We used this sampling scheme in an attempt to ensure that all wetland classes were well represented in the validation data.

Field validation points were evaluated by crews making ground-level assessments of wetland class between May and September of 2010. Geographic coordinates were acquired at each observation site using a Trimble Juno GPS data logger and the data were differentially corrected to improve positional accuracy. Image-interpretation validation points were classified using image-interpretation of high-resolution, digital stereo imagery, lidar-derived digital elevation models, and other ancillary data. Digital stereo imagery was viewed using a stereo-photogrammetry workstation equipped with StereoAnalyst software for ArcGIS (ERDAS 2010) and a Planar SD1710 stereo-mirror monitor.

The mapped wetland class was associated with the validation reference class using a spatial join process in ArcGIS. Distances to the wetland feature and class boundaries were computed. To address potential confusion between classification accuracy and positional accuracy, image-interpreted points that fell within the 95% confidence interval for the positional accuracy of the imagery (1.53 meters) of a wetland feature or class boundary were excluded from analysis. Field points that fell within the combined 95% confidence interval for the positional accuracy of the imagery and the GPS (5.64 meters) of a wetland feature or class boundary were also excluded.

The data were compared at two levels: agreement for a simple two-category system of wetland-upland features, and agreement for the wetland class-level. The producer's accuracy, the user's accuracy, and the overall accuracy were calculated (Congalton and Green 2008). The producer’s accuracy is equal to the complement to the omission error rate for the map, whereas the user’s accuracy is equal to the complement to the commission error rate. Mixed classes occur occasionally in the mapped data due to spatial scale limitations. Wetland features that consist of highly interspersed classes are impractical to separate and classify at the map scale. However, mixed classes did not occur in the validation data. For the purposes of the accuracy assessment, if the field class matched either of the classes in a mixed class map unit, it was counted as a match.

RESULTS

Intermediate Automated Classification Results

Initial image segmentation efforts resulted in many small image objects, requiring significant time spent merging, classifying, and editing features (Figure 2). However, feedback from the photo-interpreters was incorporated into a refined image segmentation rule set to provide image objects which more closely represented the wetland features of interest. Initially, the typical number of image objects per quarter quad tile was about 96,000; after refining the segmentation rules the per-tile average object count was about 4,300. The refined segmentation rules aggregated image objects resulting in an increase in the mean object size of 430 m^2 to 1,600 m^2. The minimum object area stayed roughly the same, while the maximum object area went from 8,900 m^2 to 57,000 m^2.

The subsequent random forest classification had an overall bootstrapped accuracy of 92% for separating wetlands from uplands and an overall bootstrapped accuracy of 69% for wetland class assignment. These values should be treated with some degree of caution, as the bootstrapped accuracy results are not directly comparable to the final accuracy assessment using the independent validation data. Nonetheless, these results do support the notion that the automated classification component significantly reduces the work load of the manual photo-interpreter by providing a reasonably accurate intermediate product.

Final Product Accuracy Assessment

There were 743 field validation data points after excluding points within the positional uncertainty of a mapped wetland boundary. The overall field accuracy for discriminating between wetland and upland was 90%. The wetland producer's accuracy was 90% and the user's accuracy was 96% (Table 2).

The overall accuracy at the wetland class-level was 72% (Table 3) when compared to the field validation data. Many of the discrepancies between the field class and the mapped class were the result of confusion between the limnetic (L1) and littoral (L2) systems as well as confusion between the aquatic bed (AB) and unconsolidated bottom (UB) classes.

There were 891 validation points in the image-interpreted dataset after excluding points within the positional uncertainty of the imagery of a mapped wetland boundary. The overall image-interpretation accuracy for discriminating between wetland and upland was 93% (Table 4). The wetland producer's accuracy was 93% and the user's accuracy was 98%.

The overall accuracy at the wetland class-level was 78% (Table 5) when compared to the image-interpretation validation data. As with the assessment using field data, many of the classification discrepancies were associated with confusion between the limnetic and littoral subsystems as well as confusion between the aquatic bed and unconsolidated bottom classes.

Comparison to Original NWI

The original NWI data for the 13-county project area has 125,586 wetland class features with a total surface area of 2,958 square kilometers. Whereas, the updated NWI data for the same area includes 195,983 wetland class features with a total surface area of 3,104 square kilometers; an increase of 56% for the number of wetland class features and an increase of 4.9% in wetland area. The increase in the number of individual wetland class features suggests that the updated NWI was better able to distinguish between wetland habitat classes within wetland complexes, identifying more wetland polygons with less cross-class aggregation. However, an increase of total wetland area of 4.9% over a period where urban development is widely believed to have resulted in wetland loss suggests that the updated wetland inventory also mapped many wetlands that were missed in the original inventory. A visual comparison of the results also supports this conclusion as well as clearly showing a more precise boundary placement (Figure 3).

Using our validation data, we found that present-day feature-level accuracy of the original NWI is 76% based on the image-interpreted validation data and 75% based on the field validation data (Table 6). The updated wetland inventory described here has significantly better accuracy for upland-wetland discrimination for present-day users. Likewise, the class-level accuracy for the updated NWI is also better than the original NWI for present-day users. The class-level accuracy increased by 19% based on the field validation data while it increased by 26% based on the image-interpreted validation data. To be fair, we recognize that the original NWI has a much lower accuracy at the present time in large part due to its age as well as from differences in the technical mapping approach.

DISCUSSION

Automation Efforts

Past efforts using automated classification of remote sensing data for the NWI have largely focused on the use of relatively coarse resolution, optical satellite imagery data (Tiner 1990; FGDC 1999; Ozesmi and Bauer 2002). Mapping and classifying wetlands to the Cowardin classification system used in the NWI is inherently difficult due to the number of classes, sub-classes and modifiers and the temporal variability associated with wetlands. Therefore, we opted not to attempt to fully automate the classification process; instead we designed the automation strategy around making the human image interpretation process more efficient. By automating the most time-consuming part of the image interpretations, initial delineation of boundaries and identifying broad wetland classes, we were able to allow the image interpreters to focus more of their efforts on the most difficult components of the process, such as the assignment of detailed wetland classes and modifiers.

A significant task during this project was adapting automation techniques developed in a research setting (Corcoran et al. 2011, Knight et al. 2013, Corcoran et al. 2013, Rampi et al. 2014a) for use in production over a large area. The effort allocated to building, testing and refining the automation steps required an up-front investment, but the labor saved during the image interpretation process resulted in a net gain in efficiency. Rampi et al. (2014a) used a similar automated method for a simple four-class map without subsequent manual photo-interpretation, achieving overall accuracies for wetlands in the range of 96-98 percent. These results support our assertion that the initial wetland mapping steps can be partially automated, while leaving the more detailed classification steps to human photo-interpreters. This strategy provides improvements in overall efficiency while still maintaining high standards for spatial resolution, classification detail, and accuracy.

Accuracy Assessment

The federal wetland mapping standard provides recommendations on map accuracy goals but little specific guidance on how to conduct wetland mapping accuracy assessments. There are many design decisions involved in developing an accuracy assessment method for a remote sensing wetland inventory that can influence the results. We used two different validation data sets with different methods of acquisition, one using field data and another using image-interpreted data. Simply changing the data acquisition method resulted in a difference in the overall accuracy of 3% at the feature level and 6% at the class-level. Changes in a number of other variables such as the distribution across the sampling strata or the threshold used for screening out the effects of position uncertainty would affect the calculation of final map accuracy values. Comparing accuracy results from one project to the next will be difficult without some additional standardization for the accuracy assessment method.

The federal wetland mapping standard does not address errors of commission. The standard states that 98% of all wetlands “visible on an image” and larger than 0.2 ha shall be mapped (FGDC 2009). Based on this, the producer’s accuracy for this project fell 5% short of the requirement. However, the federal wetland mapping standard only specifies a threshold for errors of omission and not errors of commission. A user’s accuracy of 98% carries no weight with respect to the federal wetland mapping standard, but clearly it is an important consideration for the end users of the data. Without specific quantification of commission errors, it is possible to bias a mapping project toward meeting the federal standards by intentionally over-classifying upland features as wetlands. The federal standard also calls for 85% attribute accuracy for wetland classes, but it is not clear whether this is intended to be a standard for the overall class accuracy or the user’s or producer’s accuracy on individual wetland classes.

There is an important relationship between class accuracy, the number of classes mapped, and how distinct these classes are. In the present case, the overall class accuracy for this project is 78%, but some of the observed classification error is certainly due to confusion between highly similar or temporally variable wetland classes. For example, the distinction between the limnetic and littoral systems is primarily based on water depth. The portion of a lacustrine system deeper than 2 meters is defined as limnetic; whereas the portion shallower than 2 meters is defined as littoral (Cowardin et al. 1979). Accurate classification of limnetic and littoral areas is very difficult without bathymetric survey data (Irish and Lillycrop 1999; Dost and Mannaerts 2008). Not only are the optical imagery, near-infrared lidar, and radar data used in this mapping effort limited in their ability to assess water depth, but also, the field validation data were acquired from shore. As a result, it is difficult to determine whether the error lies within the field data or the map data. In another example, the distinction between aquatic bed and unconsolidated bottom wetland classes is defined by the presence or absence of rooted aquatic vegetation. The confusion between these classes likely arises in large part due to the dynamic nature of aquatic vegetation. Aquatic vegetation may be present in one part of the wetland in a given year (or season within a year) and then appear in a different part of the same wetland in another year. Given the expense and difficulty associated with separating out some of the wetland classes in the Cowardin system, if a high level of accuracy for individual wetland classes is desired, it would be preferable to simplify the classification by aggregating some classes.

This mapping effort exceeded many of the input data requirements of the federal wetland mapping standard. The base imagery exceeded both the spectral and spatial resolution requirements as well as the positional accuracy requirement. The input data requirements were also exceeded by including datasets like lidar, radar, and multi-temporal imagery. Given the unusually high quality and richness of the source data used in this project, the results raise the question whether it is practically feasible to achieve the federal wetland mapping standard in large scale wetland mapping projects.

In addition to the above observations about issues with the interpretation and application of the federal wetland mapping standard, another key result from this work was to quantify the overall improvement in accuracy resulting from the update of the wetland inventory. Our results showed that when compared to current field data we achieved a 15% increase in wetland-upland discrimination and a 19% increase in wetland class accuracy. We have previously noted that this was not meant to be an assessment of the accuracy of the original NWI at the time of its creation. It seems likely that the original NWI had a higher accuracy at the time it was created. However, it is also important to note that in the absence of an updated wetland inventory, people will continue to use the original NWI to assess current conditions. Continuing to use inaccurate and outdated data results is likely to result in unnecessary effort or inadequate wetland protection. The updated NWI provides a better source of information from which to base present day natural resource management decisions.

In conclusion, we believe these results show that it is possible to produce high quality wetland inventories using a semi-automated process that will meet many, if not all, of the needs stated in the beginning of this paper. With the limited funding for these types of mapping efforts, additional work is needed to continue to increase the efficiency of wetland mapping, while at the same time producing results that meet the needs of the resource managers. Also, there is a need to refine and standardize wetland mapping accuracy assessment methods. Furthermore, detailed accuracy assessment results, such as presented here, provide important information to users who seek to understand the potential limitations of remotely sensed wetland inventory data.

ACKNOWLEDGEMENTS

Funding for this project was provided by the Minnesota Environment and Natural Resources Trust Fund as recommended by the Legislative-Citizen Commission on Minnesota Resources. The Trust Fund is a permanent fund constitutionally established by the citizens of Minnesota to assist in the *protection, conservation, preservation, and enhancement of the state's air, water, land, fish, wildlife, and other natural resources*. Special thanks to Molly Martin of the Minnesota Department of Natural Resources for technical and field assistance.

REFERENCES

Alaska Satellite Facility (2011). MapReady Remote Sensing Tool Kit Version 2.3.17 [computer software]. Available from https://www.asf.alaska.edu/data-tools/mapready/

Austin, J. E., Buhl, T. K., Guntenspergen, G. R., Norling, W., and Sklebar, H. T. (2001). Duck populations as indicators of landscape condition in the prairie pothole region. Environmental Monitoring and Assessment, 69(1), 29-48.

Baatz, M., and Schäpe, A. (2000). Multiresolution segmentation: An optimization approach for high quality multi-scale image segmentation. Angewandte Geographische Informationsverarbeitung XII (J. Strobl and T. Blaschke, editors), Wichmann, Heidelberg, pp. 12–23.

Ball Aerospace & Technologies Corp (2011). Opticks Version 4.7.1. Available from http://opticks.org

Bergeson, M.T. (2011). Wetlands Data Verification Toolset: Installation Instructions and User Information. U.S. Fish and Wildlife Service, National Standards and Support Team. Retrieved from http://www.fws.gov/wetlands/Data/tools/Wetlands-Data-Verification-Toolset-Installation-Instructions-and-User-Information.pdf

Beven, K. J., and Kirkby, M. J. (1979). A physically based, variable contributing area model of basin hydrology. Hydrological Sciences Journal, 24(1), 43-69.

Bourgeau-Chavez, L.L., Kowalski, K.P., Carlson Mazur, M.L., Scarbrough, K.A., Powell, R.B., Brooks, C.N., Huberty, B., Jenkins, L.K., Banda, E.C., Galbraith, D. M., Laubach, Z.M. and Riordan, K. (2013). Mapping Invasive Phragmites australis in the Coastal Great Lakes with ALOS PALSAR Satellite Imagery for Decision Support. Journal of Great Lakes Research, 39(1), 65-77.

Breiman, L. (2001). Random forests. Machine learning, 45(1), 5-32.

Brisco, B., Touzi, R., Van der Sanden, J., Charbonneau, F., Pultz, T., and D'Iorio, M. (2007). Water resource applications with Radarsat-2. International Journal of Digital Earth, 1(1): 130-147.

Burkett, V., and Kusler, J. (2000). Climate Change: Potential Impacts and Interactions in Wetlands of the United States. Journal of the American Water Resources Association. 36(2) 313-320.

Congalton, R. G., and Green, K. (2008). Assessing the accuracy of remotely sensed data: principles and practices. CRC press.

Corcoran, J.M, Knight, J.F., B. Brisco, S. Kaya, A. Cull, K. Murhnaghan. (2011) The integration of optical, topographic, and radar data for wetland mapping in northern Minnesota. Canadian Journal of Remote Sensing, 27(5): 564-582.

Corcoran, J.M., Knight, J.F., and Gallant, A.L. (2013) Influence of Multi-Source and Multi-Temporal Remotely Sensed and Ancillary Data on the Accuracy of Random Forest Classification of Wetlands in Northern Minnesota. Remote Sensing, 5(7): 3212-3238.

Costa, L. T., Farinha, J. C., Vives, P. T., Hecker, N., & Silva, E. P. (2001). Regional wetland inventory approaches: The Mediterranean example. In *Wetland Inventory, Assessment and Monitoring: Practical Techniques and Identification of Major Issues*. Finlayson CM, Davidson NC & Stevenson NJ (eds). Proceedings of Workshop 4, 2nd International Conference on Wetlands and Development, Dakar, Senegal, 8–14 November 1998, Supervising Scientist Report 161, Supervising Scientist, Darwin.

Cowardin, L.M., Carter, V., Golet, F.C. and LaRoe, E.T. (1979). Classification of Wetlands and Deepwater Habitats of the United States. U.S. Fish and Wildlife Service Report No. FWS/OBS/-79/31.Washington, D.C.

Dahl, T.E., Dick, J., Swords, J. and Wilen, B.O. (2009). Data Collection Requirements and Procedures for Mapping Wetland, Deepwater and Related Habitats of the United States. Division of Habitat and

Resource Conservation, National Standards and Support Team, Madison, WI. U.S. Fish and Wildlife Service 85 pp.

Definiens, A. G. (2009). Definiens eCognition Developer 8 User Guide. Definens AG, Munchen, Germany.

Drazkowski, B., May, M., and Herrera, D.T. (2004). Comparison of 1983 and 1997 Southern Michigan National Wetland Inventory Data. Michigan Department of Environmental Quality, Geological and Land Management Division. 15 pp.

Dost, R. J. J., & Mannaerts, C. M. M. (2008). Generation of lake bathymetry using sonar, satellite imagery and GIS. In *ESRI 2008: Proceedings of the 2008 ESRI International User Conference*

ERDAS (2008). ERDAS Imagine Version 9.2 [computer software]. Intergraph Corporation. Norcross, GA.

ERDAS (2010). StereoAnalyst for ArcGIS Version 10.0 [computer software]. Intergraph Corporation. Norcross, GA.

ESRI (2011). ArcGIS Desktop: Release 10 [computer software]. Environmental Systems Research Institute. Redlands, CA.

Euliss Jr, N. H., Gleason, R. A., Olness, A., McDougal, R. L., Murkin, H. R., Robarts, R. D., Bourbonniere, R.A., and Warner, B. G. (2006). North American prairie wetlands are important nonforested land-based carbon storage sites. Science of the Total Environment, 361(1), 179-188.

FGDC (2009). Wetlands mapping standard. US Geological Survey Federal Geographic Data Committee, Reston, Document Number FGDC-STD-015-2009.

Finlayson, C.M. and Spiers, A.G. (1999). Global Review of Wetland Resources and Priorities for Wetland Inventory. Supervising Scientist Report 144. Wetlands International Publication 53, Supervising Scientist, Canberra, Australia.

Frohn, R. C., Reif, M., Lane, C., and Autrey, B. (2009). Satellite remote sensing of isolated wetlands using object-oriented classification of Landsat-7 data. Wetlands, 29(3), 931-941.

Fournier, R. A., Grenier, M., Lavoie, A., & Hélie, R. (2007). Towards a strategy to implement the Canadian Wetland Inventory using satellite remote sensing. Canadian Journal of Remote Sensing, 33(S1), S1-S16.

Gong, P., Niu, Z.G., Cheng, X., Zhao, K.Y., Zhou, D.M., Guo, J.H., Liang, L., Wang, X.F., Li, D.D., Huang, H.B., Wang, Y., Wang, K., Li, W.N., Wang, X.W., Ying, Q., Yang, Z.Z., Ye, Y.F., Li, Z., Zhuang, D.F., Chi, Y.B., Zhou, H.Z. And Yan, J. (2010). China's wetland change (1990–2000) determined by remote sensing. Science China Earth Sciences, 53(7), 1036-1042.

Guisan, A., Weiss, S. B., and Weiss, A. D. (1999). GLM versus CCA spatial modeling of plant species distribution. Plant Ecology, 143(1), 107-122.

Gwin, S. E., Kentula, M. E., and Shaffer, P. W. (1999). Evaluating the effects of wetland regulation through hydrogeomorphic classification and landscape profiles. Wetlands, 19(3), 477-489.

Hepinstall, J. A., Queen, L. P., and Jordan, P. A. (1996). Application of a modified habitat suitability index model for moose. Photogrammetric engineering and remote sensing, 62(11), 1281-1286.

Hogg, A. R., and Todd, K. W. (2007). Automated discrimination of upland and wetland using terrain derivatives. Canadian Journal of Remote Sensing, 33(S1), S68-S83.

Irish, J. L., & Lillycrop, W. J. (1999). Scanning laser mapping of the coastal zone: the SHOALS system. ISPRS Journal of Photogrammetry and Remote Sensing, 54(2), 123-129.

Kloiber, S.M. (2010). Technical Procedures for the Minnesota Wetland Status and Trends Program: Wetland Quantity Assessment. Minnesota Department of Natural Resources, Division of Ecological and Water Resources Report, November 2012. 41 pp. Retrieved from

Knight, J.F., B. Tolcser, J. Corcoran, and L. Rampi. (2013) The effects of data selection and thematic detail on the accuracy of high spatial resolution wetland classifications. Photogrammetric Engineering and Remote Sensing, 79(7): 613-623.

Knutson, M. G., Sauer, J. R., Olsen, D. A., Mossman, M. J., Hemesath, L. M., and Lannoo, M. J. (1999). Effects of landscape composition and wetland fragmentation on frog and toad abundance and species richness in Iowa and Wisconsin, USA. Conservation Biology, 13(6), 1437-1446.

Li, J., and Chen, W. (2005). A rule-based method for mapping Canada's wetlands using optical, radar and DEM data. International Journal of Remote Sensing, 26(22), 5051-5069.

LMIC. (2007). (Now called Minnesota Geographic Information Office) Metadata for the National Wetlands Inventory, Minnesota. Retrieved from http://www.mngeo.state.mn.us/chouse/metadata/nwi.html

Macleod, R.D., Paige, R.S., and Smith, A.J. 2013. Updating the National Wetland Inventory in East-Central Minnesota: Technical Documentation. Minnesota Department of Natural Resources, Division of Ecological and Water Resources. St. Paul, MN. Retrieved from http://files.dnr.state.mn.us/eco/wetlands/nwi_ecmn_technical_documentation.pdf

Maidment, D. R. (Ed.). (2002). Arc Hydro: GIS for water resources (Vol. 1). ESRI, Inc. Redlands, CA.

Marchand, M. N., and Litvaitis, J. A. (2004). Effects of habitat features and landscape composition on the population structure of a common aquatic turtle in a region undergoing rapid development. Conservation Biology, 18(3), 758-767.

Minnesota Climatology Working Group. 2012. 1981-2010 Normal Precipitation Maps. Retrieved from http://www.climate.umn.edu/doc/historical/81-10_precip_norm.htm

MnGeo. 2010. Map Accuracy Report: East-Central Minnesota Ortho Project. Minnesota Geographic Information Office, St. Paul, MN. Retrieved from http://www.mngeo.state.mn.us/chouse/airphoto/2010_DOQ_Accuracy_Report_MnDOT_ecmn2010_03Jan2012.pdf

Moore, I.D., Grayson, R.B. and Ladson, A.R. (1991). Digital Terrain Modelling: A Review of Hydrological, Geomorphological, and Biological Applications. *Hydrological Processes*, **5**:3-30.

Munger, J.C., Gerber, M., Madrid, K.,Carroll, M., Petersen, W., and Heberger, L. (1998). U.S. National Wetland Inventory Classifications as Predictors of the Occurrence of Columbia Spotted Frogs (*Rana Luteiventris*) and Pacific Treefrogs (*Hylaregilla*). Conservation Biology, 12(2), 320-330.

Murphy, P. N., Ogilvie, J., Connor, K., and Arp, P. A. (2007). Mapping wetlands: a comparison of two different approaches for New Brunswick, Canada. Wetlands, 27(4), 846-854.

Myint, S.W., Gober, P., Brazel, A., Grossman-Clarke, S., and Weng, Q. (2011). Per-pixel vs. object-based classification of urban land cover extraction using high spatial resolution imagery. Remote Sensing of Environment, 115(5), 1145-1161.

NRCS (2010). Natural Resources Conservation Service, Soil Survey Staff, United States Department of Agriculture. Soil Survey Geographic (SSURGO) Database for [Anoka, Carver, Chisago, Dakota, Goodhue, Hennepin, Isanti, Ramsey, Rice, Scott, Washington, and Wright Counties, Minnesota]. Retrieved from at http://soildatamart.nrcs.usda.gov/ on 01/12/2010.

NSGIC (2014). Letter from President Kenneth Miller to the Secretary of Interior, Sally Jewell, April 16, 2014. National States Geographic Information Council.

Ozesmi, S. L., and Bauer, M. E. (2002). Satellite remote sensing of wetlands. Wetlands Ecology and Management, 10(5), 381-402.

R Development Core Team. (2011). R: A language and environment for statistical computing, reference index version 2.12. R Foundation for Statistical Computing, Vienna, Austria. ISBN 3-900051-07-0, URL http://www.R-project.org.

Rampi, L.P., Knight, J.F., and Pelletier, K.C. 2014a. Wetland mapping in the Upper Midwest United States: An object-based approach integrating lidar and imagery data. Photogrammetric Engineering and Remote Sensing. 80(5), 439-449.

Rampi, L.P., Knight, J.F., and Lenhart, C.F., 2014b. Comparison of flow direction algorithms in the application of the CTI for mapping wetlands in Minnesota. Wetlands, Feb. 2014.

Tarboton, D. G. (2003). Terrain analysis using digital elevation models in hydrology. In 23rd ESRI international users conference, San Diego, California (Vol. 14).

Tiner, R. W. (1990). Use of high-altitude aerial photography for inventorying forested wetlands in the United States. Forest Ecology and Management, 33, 593-604.

Tiner, R. W. (2009). Status report for the National Wetlands Inventory Program 2009. US Fish and Wildlife Service, Branch of Resource and Mapping Support, Arlington, VA.

Trimble (2010). eCognition Developer 8.64.0 User Guide; Trimble: Munich, Germany. 27pp.

Yerkes, T., Paige,R., Macleod, R., Armstrong, L., Soulliere, G., and Gatti, R. (2007). Predicted distribution and characteristics of wetlands used by mallard pairs in five Great Lakes States. The American Midland Naturalist. 157(2), pp. 356-364.

TABLES

Table 1

Class Code	Class Description
L1UB	Lacustrine Limnetic Unconsolidated Bottom
L2AB	Lacustrine Littoral Aquatic Bed
L2EM	Lacustrine Littoral Emergent
L2UB	Lacustrine Littoral Unconsolidated Bottom
L2US	Lacustrine Littoral Unconsolidated Shore
PAB	Palustrine Aquatic Bed
PEM	Palustrine Emergent
PFO	Palustrine Forested
PSS	Palustrine Scrub-Shrub
PUB	Palustrine Unconsolidated Bottom
R2AB	Riverine Lower Perennial Aquatic Bed
R2UB	Riverine Lower Perennial Unconsolidated Bottom
R2US	Riverine Lower Perennial Unconsolidated Shore
UPL	Upland

Table 2

	Map Determination		
Reference Determination	Upland	Wetland	Total
Upland	201	18	219
Wetland	54	470	524
Total	255	488	743

Overall Accuracy	90%
Wetland Producer's Accuracy	90%
Wetland User's Accuracy	96%

Table 3

	Map Class												
Reference Class	L1UB	L2AB	L2EM	L2UB	PAB	PEM	PFO	PSS	PUB	R2AB	R2UB	UPL	Total
L1UB	1												1
L2AB	2	14	2		2						1		21
L2EM													0
L2UB	2			21							1		24
PAB		7		2	24	3			27			5	68
PEM		1			3	130	1	3	6		1	37	182
PFO						2	22	6				24	54
PSS						8	6	18				13	45
PUB				1	3				27			3	34
R2AB											2		2
R2UB											12	3	15
UPL						6	7		1			223	237
Total	5	22	2	24	32	149	36	27	61	0	17	308	683

Table 4

	Map Determination		
Reference Determination	Upland	Wetland	Total
Upland	208	12	220
Wetland	47	624	671
Total	255	636	891

Overall Accuracy	93%
Wetland Producer's Accuracy	93%
Wetland User's Accuracy	98%

Table 5

	Map Class														
Reference Class	L1UB	L2AB	L2EM	L2UB	L2US	PAB	PEM	PFO	PSS	PUB	R2AB	R2UB	R2US	UPL	Total
L1UB	39			5								8			52
L2AB	2	26	9	3		1	4								45
L2EM															0
L2UB	5	3	3	31								3			45
L2US					1										1
PAB						21	5			11	1	1			39
PEM						2	99	2	1	1				18	123
PFO							1	30	3					19	53
PSS							13	2	20			1		7	43
PUB		1		1		22	7	1	1	142				5	180
R2AB															0
R2UB						2	2					58			62
R2US							1	1				6	6		14
UPL							5	5				1		208	219
Total	46	30	12	40	1	48	137	41	25	154	1	78	6	257	876

Table 6

	Original NWI	Updated NWI
Feature Accuracy		
Field	75%	90%
Image-interpreted	76%	93%
Class Accuracy		
Field	53%	72%
Image-interpreted	52%	78%

TABLE CAPTIONS

Table 1: Wetland class codes and associated descriptions from Cowardin et al. (1979) applicable to the study area.

Table 2: Accuracy comparison for wetland-upland discrimination using field validation data. Class agreement between the two datasets is indicated by the shaded cells in the table

Table 3: Accuracy comparison between the field validation class and the mapped wetland class in the updated NWI data. Class agreement between the two datasets is indicated by the shaded cells in the table.

Table 4: Accuracy comparison for wetland-upland discrimination using photo-interpreted validation data. Class agreement between the two datasets is indicated by the shaded cells in the table.

Table 5: Accuracy comparison between the image-interpreted validation class and the mapped wetland class in the updated NWI data. Class agreement between the two datasets is indicated by the shaded cells in the table.

Table 6: Comparison of present-day accuracy of the original NWI to the accuracy of the updated NWI.

FIGURE CAPTIONS

Figure 1: The project area includes thirteen counties in east-central Minnesota, USA.

Figure 2: Illustration of the image classification process showing (a) the infrared band from the spring imagery, (b) the lidar hillshade DEM, (c) initial image objects, (d) refined multi-resolution objects, and (e) the final wetland inventory map.

Figure 3: A comparison of the original NWI wetland boundaries (dashed black line) to the updated wetland boundaries (white line) shown on top of a lidar hillshade layer.

Figure 4 (electronic supplemental material - online only): A comparison of the original NWI wetland boundaries (green) to the updated wetland boundaries (blue) shown on top of a false color-infrared aerial image.

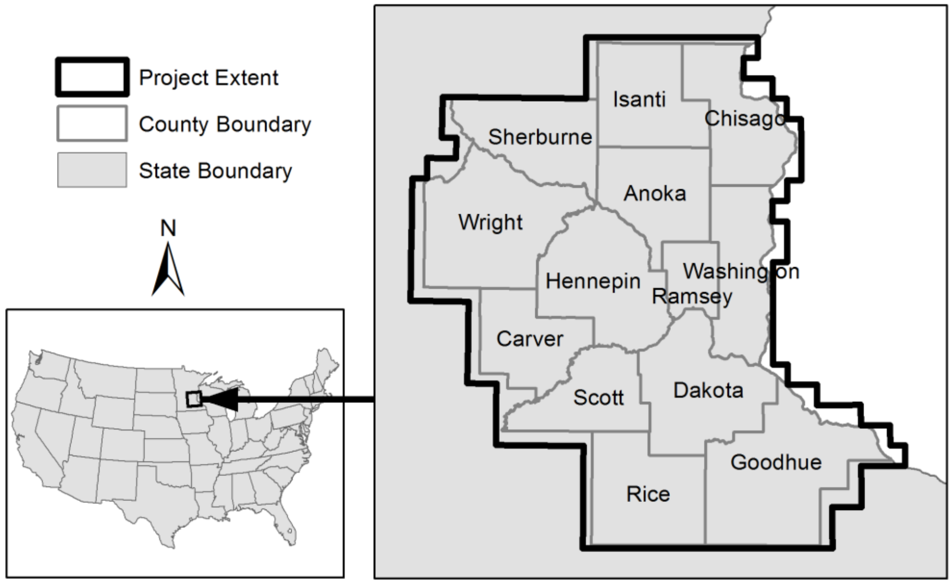

Figure 1: The project area includes thirteen counties in east-central Minnesota, USA.

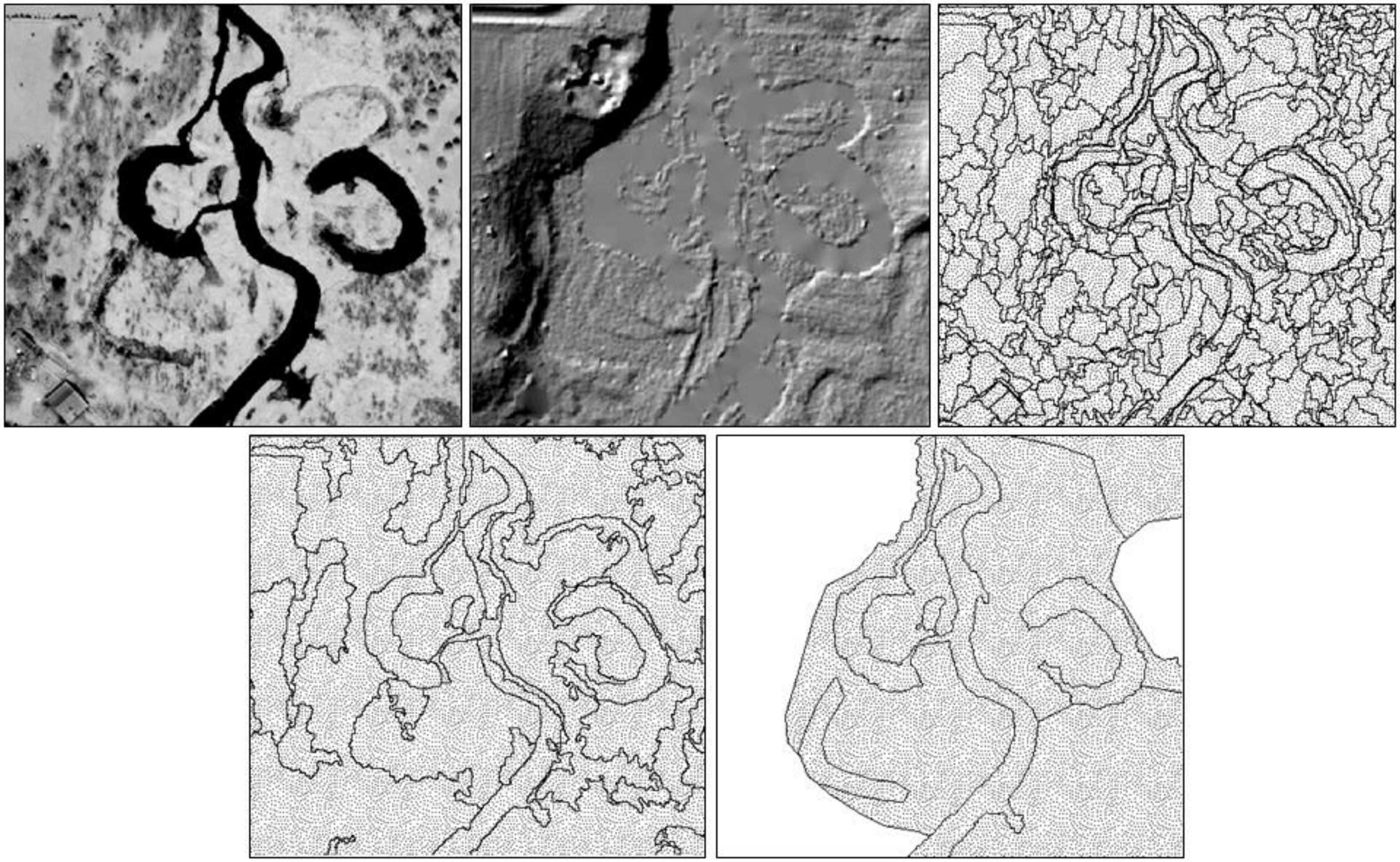

Figure 2: Illustration of the image classification process showing (a) the infrared band from the spring imagery, (b) the lidar hillshade DEM, (c) initial image objects, (d) refined multi-resolution objects, and (e) the final wetland inventory map.

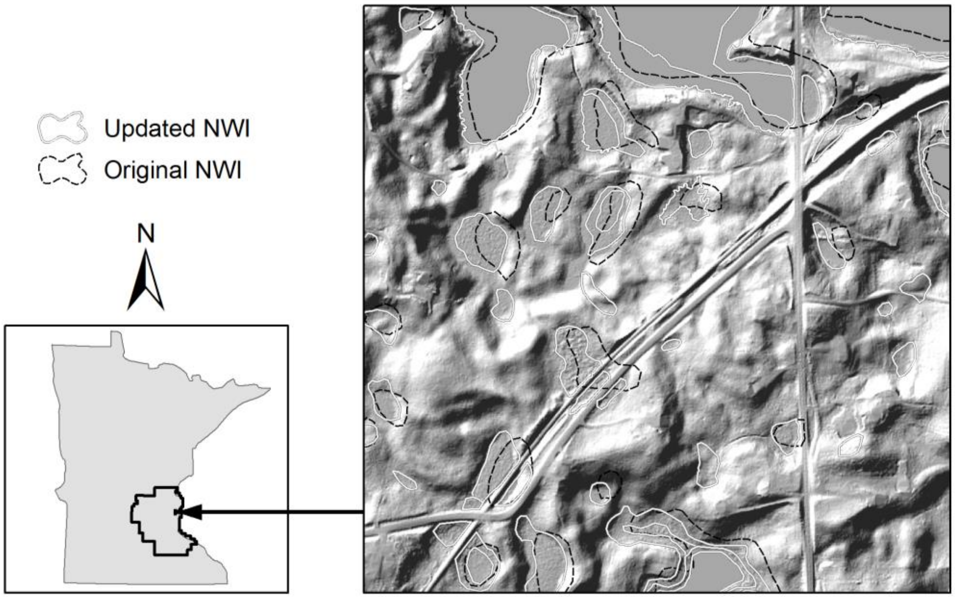

Figure 3: A comparison of the original NWI wetland boundaries (dashed black line) to the updated wetland boundaries (white line) shown on top of a lidar hillshade layer.

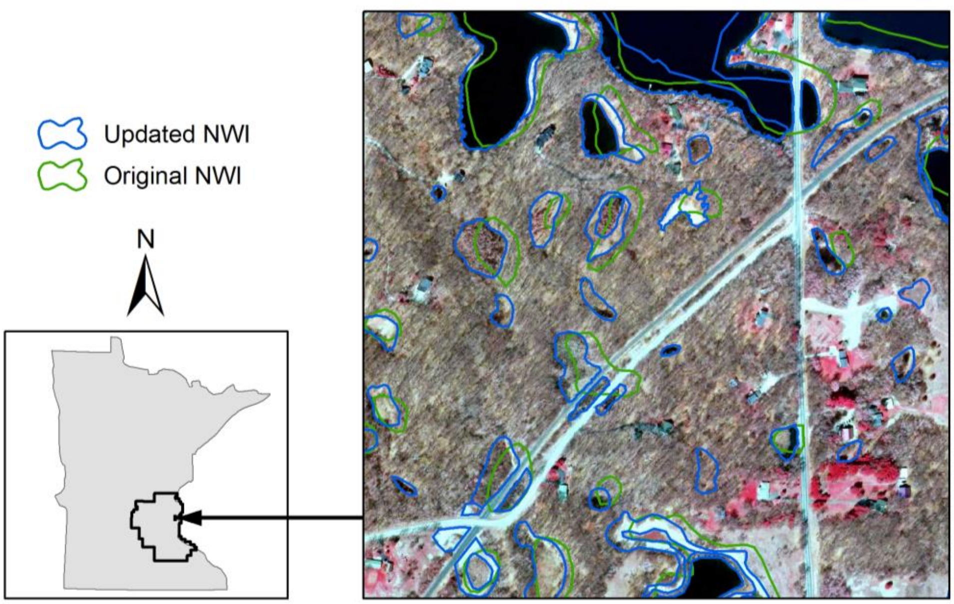

Figure 4 (electronic supplemental material - online only): A comparison of the original NWI wetland boundaries (green) to the updated wetland boundaries (blue) shown on top of a false color-infrared aerial image.